Process window and mechanism of surface property enhancement of 9Cr18 steel using plasma immersion ion implantation

Z. M. Zeng
Department of Physics and Materials Science, City University of Hong Kong, 83 Tat Chee Avenue, Kowloon, Hong Kong and Advanced Welding Production and Technology National Key Laboratory, Harbin Institute of Technology, Harbin 150001, China

B. Y. Tang and P. K. Chu[a)]
Department of Physics and Materials Science, City University of Hong Kong, 83 Tat Chee Avenue, Kowloon, Hong Kong

X. B. Tian, S. Y. Wang, and X. F. Wang
Department of Physics and Materials Science, City University of Hong Kong, 83 Tat Chee Avenue, Kowloon, Hong Kong and Advanced Welding Production and Technology National Key Laboratory, Harbin Institute of Technology, Harbin 150001, China

(Received 4 June 1998; accepted 12 November 1998)

9Cr18 martensite steel is commonly used as a bearing material in the aerospace industry in China. Because of its ability to treat large and irregular industrial components, plasma immersion ion implantation (PIII) is a good technique to enhance the wear resistance of 9Cr18 precision bearings to extend the working lifetime. We have recently conducted a systematic investigation to determine the process window of nitrogen PIII as well as to identify the enhancement mechanism. The surface properties of 9Cr18 steel after nitrogen PIII under different dosage and plasma conditions (filament hot electron discharge and radio frequency glow discharge) are evaluated by measuring the microhardness, wear property, coefficient of friction, corrosion resistance, as well as elemental depth profiles. Our data indicate that the degree of improvement does not differ substantially under the various PIII conditions thereby suggesting a fairly large process window as long as enough nitrogen is incorporated to form nitride phases. © *1999 American Vacuum Society*.
[S0734-211X(99)01902-2]

I. INTRODUCTION

9Cr18 martensitic stainless steel is often used in the Chinese aerospace industry as it possesses good corrosion resistant properties. In aerospace applications, the main mechanisms of bearing failure are surface wear and corrosion.[1] The primary reason of corrosion is that the bearings work intermittently and the lubrication oil is frequently contaminated by S, Cl, Na, K, Ca, and other deleterious elements in the working ambient. Hence, improving the surface wear and corrosion properties by surface treatment is a good way to prolong the lifetime of the bearings in the field. Because of the high Cr content of 9Cr18 steel, nitrogen ion implantation has been proposed to be a good technique to enhance the surface properties.[2]

Plasma immersion ion implantation (PIII) circumvents the line-of-sight restriction and the retained dose problem characteristic of conventional ion beam implantation.[3–7] It is therefore an excellent technique to treat large and irregular components such as aerospace bearings.[8] In this work, nitrogen PIII is utilized to treat 9Cr18 samples. We investigate the effectiveness of low pressure gas discharge and radio frequency (rf) glow discharge as well as the influence of the implant dose by comparing the microhardness, wear, and corrosion properties before and after PIII. Our results indicate unambiguously that nitrogen PIII improves these properties significantly, but the different treatment processes yield similar results. It thus appears that the process window is quite large as long as enough nitrogen is implanted to form nitride phases in the near surface region.

II. EXPERIMENT

Test coupons of 9Cr18 bearing steel (composition in wt %: Fe-79.655, Si-0.8, Mn-0.72, P-0.035, S-0.03, C-0.96, and Cr-17.8) in the quenched-and-tempered state often used in bearing applications were studied. The samples to be implanted received a final polish to a surface roughness, R_a, of 0.04 μm, and were cleaned ultrasonically in acetone. Nitrogen PIII was carried out in a multipurpose plasma immersion ion implanter.[9] The nitrogen plasma was generated by two different means: (i) low pressure gas discharge by hot electrons emitted from heated filaments and (ii) radio-frequency glow discharge using a 13.56 MHz, 2 kW rf inductively coupled plasma source. The samples were mounted on an oil-cooled stage to keep them at close to room temperature during PIII in an effort to eliminate the temperature factor that is expected to be different under the two plasma excitation conditions if no sample cooling is implemented. Prior to nitrogen implantation, the samples were sputter cleaned in an argon plasma for 15 min. The instrumental conditions are summarized in Table I.

The coefficient of friction was measured on a pin-on-disk wear tester equipped with a ruby ball 3 mm in diameter. The

[a)]Corresponding author; electronic mail: paul.chu@cityu.edu.hk

TABLE I. Experimental conditions.

Sample No.	0	1	2	3	4
Plasma generation method	none	rf glow discharge	rf glow discharge	Filament gas discharge	Filament gas discharge
Implantation voltage		32 kV	32 kV	32 kV	32 kV
Pulse width		30 μs	30 μs	30 μs	30 μs
Pulse repetition rate		300 Hz	300 Hz	300 Hz	300 Hz
rf power		500 W	500 W		
Discharge voltage				80 V	80 V
Discharge current				0.8 A	0.8 A
Pressure		4×10^{-1} Pa	4×10^{-1} Pa	2×10^{-2} Pa	2×10^{-2} Pa
Dose (at./cm^2)	untreated	2×10^{17}	5×10^{17}	2×10^{17}	5×10^{17}

tests were conducted using a load of 30 g and sliding speed of 1×10^{-3} m/s. An HX-1000 tester was operated with a loading of 25 g to obtain the microhardness of each sample. Polarization curves were measured in 0.1 M NaCl buffer solution and 0.1 M H_2SO_4 solution to evaluate the corrosion properties of the samples. Chemical analyses of the implanted layers were performed by x-ray photoelectron spectroscopy (XPS) and elemental depth profiles were acquired by Auger electron spectroscopy (AES).

III. RESULTS AND DISCUSSION

Table II shows the dramatic improvement in the microhardness after nitrogen PIII under various conditions. The samples implanted using a radio frequency plasma source (sample Nos. 1 and 2) exhibit slightly better properties which can be attributed to the higher plasma density and chemical activity of the rf plasma. A comparison of the friction behavior of the five samples is displayed in Fig. 1. The unimplanted sample has a relatively high friction coefficient (0.8–0.9), and at the beginning of the test, the friction coefficient is lower due to the existence of a small amount of water and adsorbates on the surface. As this layer is punched through during the test, the friction coefficient increases precipitously after 450 cycles. In comparison, for the PIII sample, the friction coefficient starts out at a lower value (0.1–0.3) because an implanted layer with lower friction has been formed on the surface. As the test proceeds, i.e., increasing rotating cycles, the implanted layer is damaged and the substrate is exposed. The friction coefficient increases to the same value (0.8–0.9) of the unimplanted specimen (sample No. 0). We can define the ''cut-through'' cycle number as the number of rotating cycles after which the implanted layer is damaged and the friction coefficient begins to increase. The cut-through cycle of each sample is depicted in Table II. The wear property is improved considerably after nitrogen PIII and as expected, a higher implantation dose gives rise to a larger cut-through cycle. However, the type of plasma excitation source has a less pronounced effect, and in fact, the samples treated by filament discharge show higher cut-through cycles contrary to the microhardness values. This is perhaps due to the slightly higher implantation temperature during filament PIII and consequently enhanced diffusion of the nitrogen atoms as a result of inefficient sample cooling.

TABLE II. Microhardness and cut-through cycle numbers of the five samples.

Sample No.	Microhardness (HV)	Cut-through cycle numbers
0	430	450
1	577	3260
2	598	9600
3	490	4200
4	550	10 800

The high resolution XPS Cr 2*p* and N 1*s* spectra acquired from one of the implanted samples are displayed in Fig. 2. The peak at 575.9 eV indicates the formation of chromium nitride after PIII. The N 1*s* spectrum shows three different chemical states of nitrogen. Based on published binding energies in the literature, the main peak at 396.2 eV corresponds to CrN. Therefore, the implanted nitrogen has formed primarily chromium nitride bonds. The other two small peaks corresponding to binding energies of 399.4 and 403.7 eV reveal that a small amount of nitrogen exists in other chemical states. Nonetheless, from the XPS results, the CrN phase is dominant after nitrogen PIII and is believed to be responsible for the improvement in the microhardness and wear properties. Figure 3 shows the Auger depth profile of an implanted PIII 9Cr18 bearing steel sample. The nitrogen profile displays a Gaussian distribution. There is also a certain amount of surface oxygen attributable to residual gas contamination in the PIII chamber.

The anode polarization curves of the five 9Cr18 samples

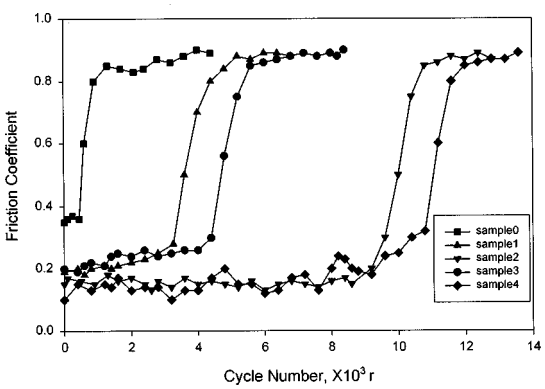

FIG. 1. Coefficient of friction curves of the 9Cr18 samples.

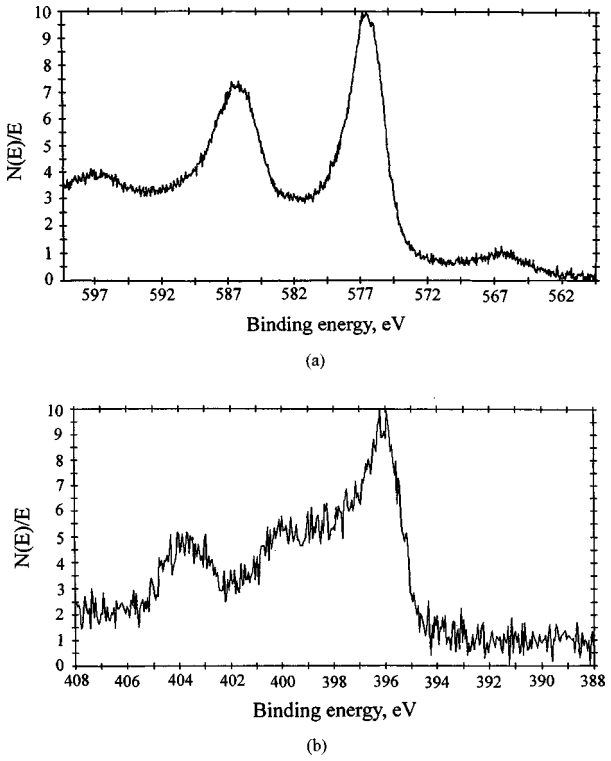

FIG. 2. XPS results of the nitrogen-implanted 9Cr18 sample—(a) Cr 2*p* spectrum, (b) N 1*s* spectrum.

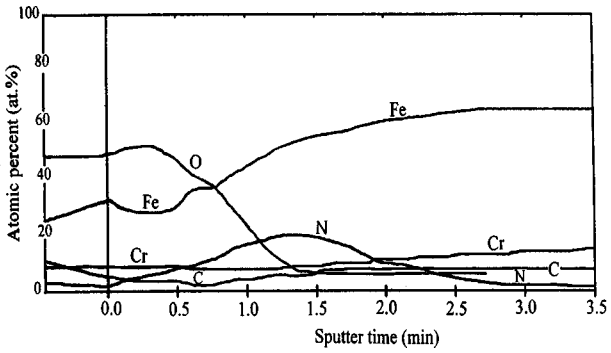

FIG. 3. AES depth profile of a nitrogen-implanted 9Cr18 sample.

in 0.1 M NaCl buffer solution and 0.1 M H_2SO_4 solution are shown in Figs. 4 and 5. According to the Tafel relation derivation method, we can obtain the corrosion current and corrosion potential of each sample. The corrosion resistance, corrosion current density, and corrosion potential are listed in Tables III and IV. It can be observed that the corrosion potentials of the implanted samples are higher than that of the untreated sample both in NaCl and H_2SO_4 solutions. This demonstrates unambiguously the improvement of the surface chemical stability after PIII. The difference in the corrosion current density among the four treated samples (samples Nos. 1 to 4) is not very big. In addition, different implant doses and plasma excitation methods do not affect the electrochemical corrosion curves significantly. Our data thus imply that a nitrogen implanted layer plays a crucial role in improving the electrochemical behavior of 9Cr18 steel, but how it is formed is not as important. We believe that nitride phases formed in the implanted layer are most critical as demonstrated by the high anode potential, even though it has also been suggested that air-formed oxide after nitrogen ion implantation also plays an important role in improving the electrochemical behavior of nitrogen implanted steel.[2,10]

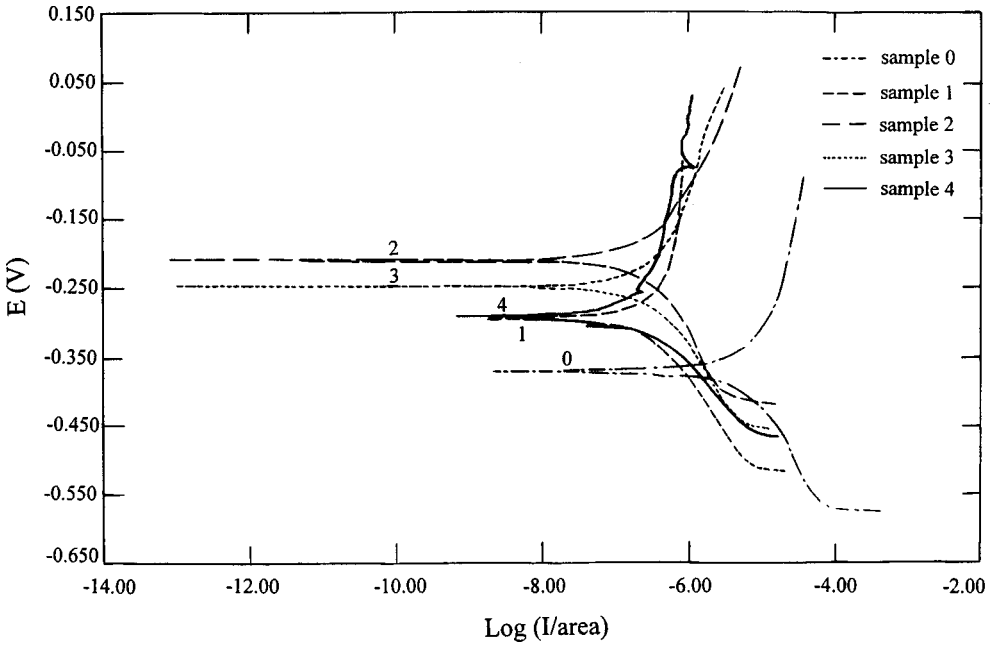

FIG. 4. Anode polarization curves in NaCl solution.

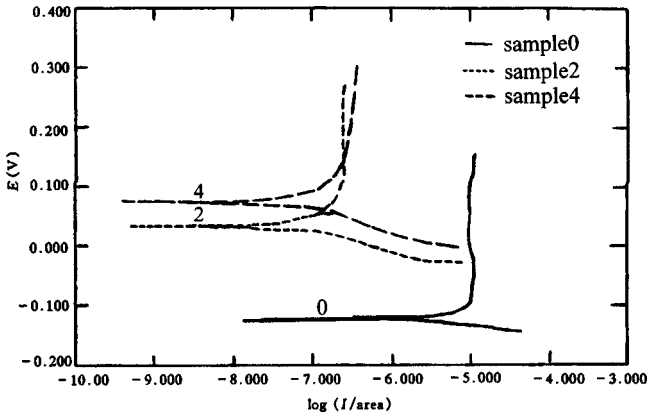

FIG. 5. Anode polarization curves in H_2SO_4 solution.

TABLE III. Results of electrochemical corrosion test in NaCl solution.

Sample No.	Corrosion resistance (kΩ)	Corrosion current density (μA/cm^2)	Corrosion potential (V)
0	5.348	4.060	−0.3703
1	85.09	0.2552	−0.2953
2	129.30	0.1680	−0.2104
3	111.90	0.1940	−0.2497
4	128.30	0.1692	−0.2925

TABLE IV. Results of electrochemical corrosion test in H_2SO_4 solution.

Sample No.	Corrosion resistance (kΩ)	Corrosion current density (μA/cm^2)	Corrosion potential (V)
0	0.4499	21.13	−0.074
2	60.58	0.1792	+0.035
4	60.08	0.1807	+0.075

IV. CONCLUSION

Nitrogen plasma immersion ion implantation enhances the microhardness and wear properties of 9Cr18 steel. The surface friction and corrosion resistance are also improved dramatically. Our experimental results indicate that the degree of enhancement does not differ significantly under different dosage and plasma conditions. Hence, it appears that the process window of 9Cr18 PIII treatment is quite large as long as enough nitrogen is implanted into the materials to form nitride phases. PIII is thus a viable technique to treat industrial and aerospace components made of 9Cr18 steel.

ACKNOWLEDGMENTS

The work is financially supported by City University of Hong Kong Strategic Grants 7000730 and Hong Kong Research Grants Council Earmarked Grant Nos. 9040332 and 9040344.

[1]Y. R. Wang *et al.*, Aerospace Manufacturing Eng. **5**, 16 (1993).
[2]T. M. Wang, B. Q. Li, and J. Shi, Surf. Coat. Technol. **50**, 63 (1991).
[3]J. R. Conrad, S. Baumann, R. Fleming, and G. P. Meeker, J. Appl. Phys. **65**, 1707 (1989).
[4]A. Chen, J. T. Scheuer, C. Ritter, R. B. Alexander, and J. R. Conrad, J. Appl. Phys. **70**, 6757 (1991).
[5]P. K. Chu, S. Qin, C. Chan, N. W. Cheung, and L. A. Larson, Mater Sci. Eng. R. **17(6-7)**, 207 (1996).
[6]S. Y. Wang, P. K. Chu, B. Y. Tang, X. C. Zeng, Y. B. Chen, and X. F. Wang, Surf. Coat. Technol. **93**, 309 (1997).
[7]J. R. Conrad, J. L. Radtke, R. A. Dodd, F. J. Worzala, and N. E. Tran, J. Appl. Phys. **62**, 4591 (1987).
[8]S. Y. Wang, P. K. Chu, B. Y. Tang, X. C. Zeng, and X. F. Wang, Nucl. Instrum. Methods Phys. Res. B **127**, 100 (1997).
[9]P. K. Chu, B. Y. Tang, Y. C. Cheng, and P. K. Ko, Rev. Sci. Instrum. **68**, 1866 (1997).
[10]C. R. Clayton, Nucl. Instrum. Methods **182**, 865 (1981).